Research on Three-phase Optimal Power Flow for Distribution Networks Based on Constant Hessian Matrix

Zhao Fengzhan[1], Zhao Tingting[1], Ju Yuntao[1*], Ma Kang[2], Zhou Xianfei[3]

[1] College of Information and Electrical Engineering, China Agricultural University, Beijing, China,
[2] Department of Electronic and Electrical Engineering, University of Bath, UK,
[3] State Grid Beijing Electronic Power Company, Beijing, China.
[*]Email: juyuntao@cau.edu.cn

Abstract: The optimal power flow (OPF) problem for active distribution networks with distributed generation (DG) and a variety of discretely adjustable devices (e.g., on-load tap-changers, OLTCs) is essentially a non-convex, nonlinear, mixed-integer optimization problem. In this paper, the quadratic model of three-phase OLTCs is proposed by adding branch currents as unknown variables, which guarantee a constant Hessian matrix throughout iterations. This paper proposes a three-phase OPF model for active distribution networks, considering a three-phase DG model. The OPF model is solved by an interior point method incorporating a quadratic penalty function as opposed to a Gaussian penalty function. Furthermore, a voltage regulator is also incorporated into the OPF model to form an integrated regulation strategy. The methodology is tested and validated on the IEEE 13-bus three-phase unbalanced test system.

1. Introduction

The optimal power flow (OPF) for active distribution networks with distributed generation (DG) and a variety of discretely adjustable devices is a non-convex, non-linear, mixed-integer optimization problem. It involves both discrete and continuous variables. By optimizing the operation strategy of the adjustable devices, including shunt capacitors, adjustable distributed energy resources, on-load tap-changers (OLTCs), etc., the OPF aims to minimize the operation cost which takes into account network losses. DG and energy storage units bring new challenges to traditional OPF problems [1-7]. Reference [6] studied how the uncertainty in wind outputs and the correlation among multiple wind farms would affect the OPF. Reference [6] did not consider discrete adjustable devices, which are prevalent in active distribution networks. Reference [7] proposed an OPF model for active distribution networks with OLTCs, where a piecewise linear model is adopted to model OLTCs. The OPF is solved by a second-order cone relaxation method [7]. Reference [8] optimizes the operation of an active distribution network where a non-coupled model is adopted for DG, yielding approximate results. Reference [9] proposed a three-phase steady-state model for DG – the model can be applied to OPF for active distribution networks.

The primal-dual interior point method has been widely used to solve the OPF problem for traditional power systems because of its advantages such as efficiency and fast convergence [10-20]. Reference [13] proposed a discrete variable processing method based on the Gaussian penalty function, but it does not compare the computation efficiency of the function with that of other penalty functions, e.g., the quadratic penalty function as introduced in [20]. By introducing a virtual node into the OLTC model, reference [14] transformed the OPF model into a quadratic optimization in the Cartesian coordinate system, thus improving computation efficiency.

This paper proposes a new asymmetrical injection model for DG with three phase coupling and a new quadratic model for three-phase OLTCs. The three-phase OPF for active distribution networks is solved by a predictor-corrector primal-dual interior point method (PCPDIPM) incorporating a penalty function. The network voltages are fine-tuned on each phase by a voltage regulator, and an integrated regulation strategy is proposed and incorporated into the OPF problem so that the voltages are fine-tuned on each phase to further optimize the network loss. Case studies demonstrate that the quadratic models for three-phase OLTCs and DG improve both the computation efficiency and the accuracy of the OPF. Case studies also compared the advantages and disadvantages of 1) the Gaussian penalty function; and 2) the quadratic penalty function with continuous variable discretization process. The impacts of the voltage regulator on nodal voltages and network losses are also demonstrated.

2. Three-Phase Distribution Networks

2.1. Quadratic model of three-phase OLTCs

In the Cartesian coordinate system, the OPF model is a nonlinear optimization problem with an order higher than quadratic if considering the turns ratio of the OLTC as a control variable. When solving the OPF problem by the interior point method, the Hessian matrix is updated in each iteration, bringing about significant computation burden [14][21]. In order to solve this problem, a new three-phase OLTC model is proposed in this paper. By adding the branch currents as state variables, the Hessian matrix becomes constant throughout the iterations of the OPF.

Fig.1 shows the OLTC in a Wye-delta (Yd) configuration, a virtual node *m* is added to branch *ij*. This transforms the OLTC into an ideal transformer *im* (with an adjustable turns ratio *k*) connected in series with an equivalent impedance *mj* (with impedance $R + jX$). The nodal voltages and branch currents are also shown in Fig.1.

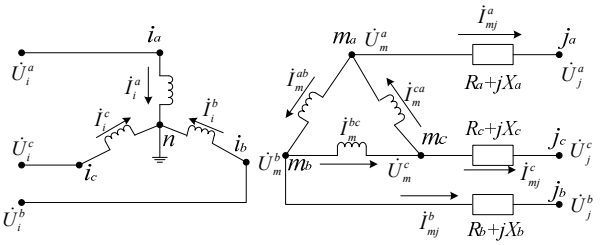

Fig.1. *Three-Phase Model of OLTCs*

With the ideal transformer, there is

$$\begin{cases} \dot{U}_i^a = k(\dot{U}_m^a - \dot{U}_m^b) \\ \dot{U}_i^b = k(\dot{U}_m^b - \dot{U}_m^c) \\ \dot{U}_i^c = k(\dot{U}_m^c - \dot{U}_m^a) \end{cases} \tag{1}$$

Based on the conservation of energy, there is

$$\begin{cases} \dot{U}_i^a \left(\dot{I}_i^a\right)^* + (\dot{U}_m^a - \dot{U}_m^b)\left(\dot{I}_m^{ab}\right)^* = 0 \\ \dot{U}_i^b \left(\dot{I}_i^b\right)^* + (\dot{U}_m^b - \dot{U}_m^c)\left(\dot{I}_m^{bc}\right)^* = 0 \\ \dot{U}_i^c \left(\dot{I}_i^c\right)^* + (\dot{U}_m^c - \dot{U}_m^a)\left(\dot{I}_m^{ca}\right)^* = 0 \end{cases} \tag{2}$$

Substituting (1) in (2) yields,

$$\begin{cases} k\dot{I}_i^a = -\dot{I}_m^{ab} \\ k\dot{I}_i^b = -\dot{I}_m^{bc} \\ k\dot{I}_i^c = -\dot{I}_m^{ca} \end{cases} \tag{3}$$

In the three-phase system, the line voltage is set as the base voltage. So, for the Yd transformer, the standard transformation ratio is 1: $\sqrt{3}$ under the per-unit system.

Considering the equivalent impedance branch *mj*, there is

$$\begin{cases} \dot{U}_m^a - \dot{U}_j^a = \dot{I}_{mj}^a (R_a + jX_a) \\ \dot{U}_m^b - \dot{U}_j^b = \dot{I}_{mj}^b (R_b + jX_b) \\ \dot{U}_m^c - \dot{U}_j^c = \dot{I}_{mj}^c (R_c + jX_c) \end{cases} \tag{4}$$

2.2. *Quadratic model of three-phase DGs*

The model in Fig. 2 represents different types of DG units, including those with the interface of voltage-source converters, wind generation based on doubly fed induction generators, synchronous generators, etc.

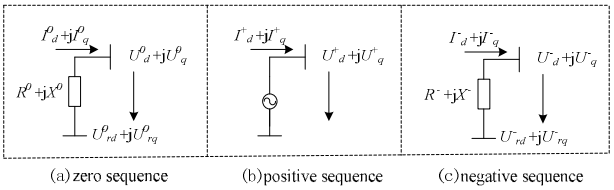

Fig.2. *A generalized sequence component model of DG*

Where I^0_d+jI^0_q, I^+_d+jI^+_q, and I^-_d+jI^-_q represent zero sequence current, positive sequence current, and negative sequence current from DG to the network, respectively. U^0_d+jU^0_q, U^+_d+jU^+_q, and U^-_d+jU^-_q represent zero sequence voltage, positive sequence voltage, and negative sequence voltage at the coupling point, respectively. R^0+jX^0 and R^-+jX^- represent zero sequence impedance and negative sequence impedance, respectively. U^0_{rd}+jU^0_{rq} and U^-_{rd}+jU^-_{rq} represent the zero sequence and negative sequence of the excitation voltage, respectively.

The DG control system consists of three parts: active power control, reactive or voltage control, and the control of the unbalanced components. The active power control keeps the positive sequence active power unchanged. The reactive control maintains a constant reactive power injection to the grid. DG excitation voltage contains only positive sequence component, with negative and zero sequence components being zero. Consequently, the equality constraints are established, as shown in equations (5, 6, 7).

$$\mathrm{Re}\left[(U_d^+ + jU_q^+)(I_d^+ - jI_q^+)\right] = U_d^+ I_d^+ + U_q^+ I_q^+ = P_{sp} \tag{5}$$

$$\mathrm{Im}\left[(U_d^+ + jU_q^+)(I_d^+ - jI_q^+)\right] = U_q^+ I_d^+ - U_d^+ I_q^+ = Q_{sp} \tag{6}$$

$$\begin{cases} U_{rd}^0 = \mathrm{Re}\left[(I_d^0 + jI_q^0)(R^0 + jX^0) + U_d^0 + jU_q^0\right] = 0 \\ U_{rq}^0 = \mathrm{Im}\left[(I_d^0 + jI_q^0)(R^0 + jX^0) + U_d^0 + jU_q^0\right] = 0 \\ U_{rd}^- = \mathrm{Re}\left[(I_d^- + jI_q^-)(R^- + jX^-) + U_d^- + jU_q^-\right] = 0 \\ U_{rq}^- = \mathrm{Im}\left[(I_d^- + jI_q^-)(R^- + jX^-) + U_d^- + jU_q^-\right] = 0 \end{cases} \tag{7}$$

Where, Re[] and Im[] correspond to the real part and the imaginary part of the expression, respectively. P_{sp} and Q_{sp} correspond to the positive sequence values of the target active power and reactive power, respectively.

The grid interface of a three-phase coupled DG is modelled as both a voltage controlled voltage source and a current controlled current source, as illustrated in Fig. 3. The sequence values of the DG injection currents and the terminal voltages are unknown variables in the quadratic model of DG. The variables include $\dot{U}^0$, $\dot{U}^+$, $\dot{U}^-$, $\dot{I}^0$, $\dot{I}^+$, $\dot{I}^-$.

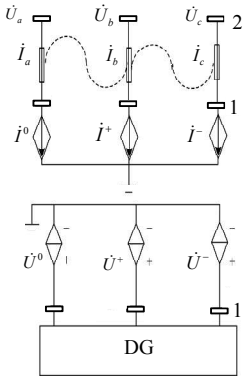

Fig.3. *Sequence-phase coupled interface*

The transformations from phase values to sequence values are given by

$$\left[\dot{U}^0 \quad \dot{U} \quad \dot{U}^-\right]^T = T_{abc\to 0+-}\left[\dot{U}_a \quad \dot{U}_b \quad \dot{U}_c\right]^T \quad (8)$$

$$\left[\dot{I}^0 \quad \dot{I}^+ \quad \dot{I}^-\right]^T = T_{abc\to 0+-}\left[\dot{I}_a \quad \dot{I}_b \quad \dot{I}_c\right]^T \quad (9)$$

Where, $T_{abc\to 0+-}$ is phase to sequence transformation matrix. ' • ' corresponds to complex quantities.

The constraints (5) – (9) consider the coupling characteristics of three-phase powers. They are different from the steady-state model in [22] which does not consider sequence control under unbalanced condition. The equations involving DG are either linear or quadratic – this guarantees a constant Hessian matrix in the OPF.

A popular model of DG is the three-phase non-coupling model [8], described in (10).

$$P^P + jQ^P = (U^P_{re} + jU^P_{im})(I^P_{re} - jI^P_{im}) \quad (10)$$

Where, P^P and Q^P correspond to the active and reactive power outputs from DG on phase P, respectively. U^P_{re} and U^P_{im} correspond to the real part and the imaginary part of the nodal voltage of DG on phase P, respectively. I^P_{re} and I^P_{im} correspond to the real part and the imaginary part of the injection current from DG on phase P, respectively.

The three-phase coupled model of DG is accurate model, and the three-phase non-coupled model is an approximate model. So, the optimal power flow results of the three-phase coupled model are more accurate than those of the approximate three-phase non-coupled model.

The above formulas constitute the DG constraints in the three-phase OPF model. Since the highest order of these formulas are quadratic, the Hessian matrix is constant throughout iterations.

2.3. Three-phase model of voltage regulator

A voltage regulator is connected to the grid for the fine-tuning of nodal voltages. A three-phase Y-connected voltage regulator consists of three single-phase voltage regulators, each with a tap changer that changes the tap position. The configuration of the three-phase voltage regulator is illustrated in Fig.4.

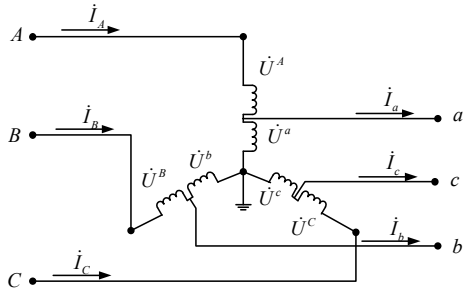

Fig.4. *Three-phase star-shaped voltage regulator*

The following constraints apply:

$$\begin{cases} \dot{U}^A = k_a\dot{U}^a \\ \dot{U}^B = k_b\dot{U}^b \\ \dot{U}^C = k_c\dot{U}^c \end{cases} \quad (11)$$

$$\begin{cases} k_a\dot{I}^A = \dot{I}^a \\ k_b\dot{I}^B = \dot{I}^b \\ k_c\dot{I}^C = \dot{I}^c \end{cases} \quad (12)$$

$$\begin{cases} k_a = 1 \pm 0.00625 \times Tap_a \\ k_b = 1 \pm 0.00625 \times Tap_b \\ k_c = 1 \pm 0.00625 \times Tap_c \end{cases} \quad (13)$$

In formula (13), a plus ('+') corresponds to 'step up' and a minus ('—') corresponds to 'step down'. '*Tap*' denotes the position of voltage regulator tap (e.g., 32-level adjustments within a range of ±10%). The tap is controlled to regulate the voltage of load center with a line voltage drop compensator. The line voltage drop compensator is coupled with the distribution line through a voltage transformer (turns ratio N_{PT}: 1) and a current transformer (turns ratio C_{TP}: C_{TS}), as shown in Fig.5. The impedance of the compensator represents the equivalent impedance from the regulator to the load center:

$$R' + jX' = (R + jX)\frac{CT_P}{N_{PT}} \quad (14)$$

The voltage at the load center is

$$\dot{U}^x_{load} = \dot{U}^x / N_{PT} - (R' + jX') \cdot \dot{I}^x / CT_P \quad (15)$$

If the voltage level of the load center is 120V and the bandwidth is 2V, the voltage will change by 0.75V each time the tap of the voltage regulator moves to the next position. The step up and the step down tap changes are given by

$$Tap_x = \frac{119 - U^x_{load}}{0.75} \quad (16)$$

$$Tap_x = \frac{U^x_{load} - 121}{0.75} \quad (17)$$

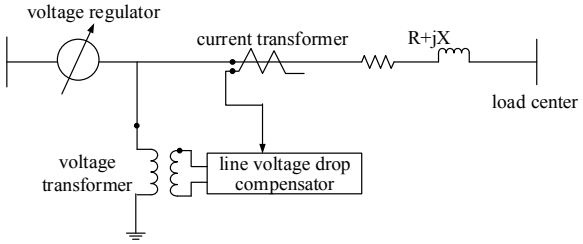

Fig.5. *Line voltage drop compensator*

3. Optimal Power Flow Model and Algorithm

3.1. OPF model

This paper establishes three-phase OPF model for distribution networks by taking the nodal voltages and branch currents as the state variables.

The objective function of the OPF model is the minimum loss of the network, as shown in equation (18).

$$\min f(x) = P_{loss} = \sum_{br=1}^{bn}\sum_{P=\{A,B,C\}} \dot{U}_{br,P}\dot{I}^*_{br,P}\Delta t \quad (18)$$

Where, *bn* is the number of branches in the network. $U_{br,P}$ and $I_{br,P}$ correspond to the branch voltage and branch current on phase P of the br_{th} branch, respectively. And the branch voltage is the difference between the nodal voltages at both ends of the branch.

The equations include the KCL and KVL constraints (as shown in equation (19)), transformer branch constraints (as shown in equation (1) (3) (4)), DG branch constraints (such as (5) - (9)), the regulator branch constraints (as shown in equation (11) (12)).

$$\begin{aligned} \mathbf{U}_{br,P,re} &= \mathbf{A}\mathbf{U}_{n,P,re} \\ \mathbf{U}_{br,P,im} &= \mathbf{A}\mathbf{U}_{n,P,im} \\ 0 &= \mathbf{A}^T\mathbf{I}_{br,P,re} \\ 0 &= \mathbf{A}^T\mathbf{I}_{br,P,im} \end{aligned} \tag{19}$$

Where, $U_{br,P,re}$ and $U_{br,P,im}$ correspond to the real part and the imaginary part of the branch voltage on phase P of the br_{th} branch, respectively. $U_{n,P,re}$ and $U_{n,P,im}$ correspond to the real part and the imaginary part of the nodal voltage on phase P of the n_{th} node, respectively. $I_{br,P,re}$ and $I_{br,P,im}$ correspond to the real part and the imaginary part of the branch current on phase P of the br_{th} branch, respectively. A is the node-branch incidence matrix

The inequality constraints include state variable constraints and control variable constraints. The state variable constraints include the generator active and reactive power constraints, the node voltage amplitude constraint, and the line transmission power P_{ij} constraint (as shown in equation (20)). The control variable constraints including the constraints of the OLTC turns ratio K_{T}, the voltage regulator tap position K_{V}, reactive power capacitor compensation capacity Q_{C}, as shown in equation (21).

$$\begin{aligned} &\underline{P}_{Gi,P} \le P_{Gi,P} \le \overline{P}_{Gi,P} \\ &\underline{Q}_{Gi,P} \le Q_{Gi,P} \le \overline{Q}_{Gi,P} \\ &\underline{U}^2_{i,P} \le U^2_{i,P,re} + U^2_{i,P,im} \le \overline{U}^2_{i,P} \end{aligned} \tag{20}$$

$$\begin{aligned} &\underline{K}_{T,i} \le K_{T,i} \le \overline{K}_{T,i} \\ &\underline{K}_{V,i} \le K_{V,i} \le \overline{K}_{V,i} \\ &\underline{Q}_{C,i} \le Q_{C,i} \le \overline{Q}_{C,i} \end{aligned} \tag{21}$$

Thus, the equations in the OPF model are either linear or quadratic which guarantees a constant Hessian matrix when the interior point method is used to solve the model. In this paper, we use the predictor-corrector primal-dual interior point method [23] to solve the optimization model with the advantages of efficiency and fast convergence.

3.2. Continuous variable discretization process

The OPF for active distribution networks involves discrete control variables (such as OLTCs turns ratio, capacitor compensation capacity, etc.). The objective function incorporates a penalty function to cope with the discrete variables. This introduces a virtual loss to the objective function which will reduce the error brought by rounding-off. At present, the quadratic penalty function [20] and the Gaussian penalty function [13] are two widely used penalty functions, as given by (22) and (23), respectively.

$$\phi(x) = \frac{1}{2}\sum_{i=1}^{n} v(x_i - b_i)^2 \tag{22}$$

$$\phi(x) = vG(x) = v\exp[-\sum_{i=1}^{n}\frac{(x_i - b_i)^2}{c_i}] \tag{23}$$

Where v is penalty factor. The value of the function drops to zero when the distance from the vector $x = (x_1, x_2, \ldots, x_n)^T$ to the center $b = (b_1, b_2, \ldots, b_n)^T$ reduces to zero.

The penalty function is incorporated into (18),

$$\min P_{loss} = \sum_{br=1}^{bn}\sum_{P=\{A,B,C\}} \dot{U}_{br,P}\dot{I}_{br,P}^{*}\Delta t + \phi \tag{24}$$

When the penalty factor is large enough, the discrete control variable will be optimized to the corresponding discrete value, so that the penalty function value becomes zero and the objective function to reach the minimum value.

Compared with the quadratic penalty function, the Gaussian penalty function decreases faster than the quadratic penalty function with the decrease of the distance between the vectors x and b; the former is more sensitive to the variation of discrete variables. However, the Gaussian penalty function is a non-quadratic function, which makes the Hessian matrix change throughout iterations — this compromises computation efficiency.

3.3. Integrated regulatory strategy

In order to minimize network losses, this paper proposes an OPF integrated regulatory strategy with voltage regulators. The integrated regulatory strategy is defined as an OPF strategy for a variety of adjustable devices to coordinate and optimize in this paper — the voltage regulator fine-tunes nodal voltages on each phase, and constitutes integrated regulatory strategy with the generator, OLTCs, shunt capacitors and DGs.

The voltage regulator is a special transformer with a zero equivalent impedance. The voltage regulator is modelled by a quadratic model where the tap position is chosen as a control variable. The Hessian matrix remains constant under the integrated regulatory strategy. This is the reason why the integrated regulatory strategy is suitable for the OPF model proposed in this paper.

4. Example

According to the three-phase OPF model for distribution networks based on constant Hessian matrix, this paper uses Symbolic Math Toolbox to verify the model on MATLAB. And the OPF analysis is carried out on the modified IEEE13 test system as shown in Fig.6. The mutual-impedance and the mutual-admittance are omitted in the figure. The control variables in the example are generator reactive power, DG output, the turns ratio of the OLTC, voltage regulator tap position and capacitors adjustment, in which the turns ratio of the OLTC and the capacitors are discrete control variables. The range of the turns ratio is set at 0.90~1.10, divided into 8 taps, its step

size is 0.025. The maximum reactive power of the capacitors is 0.02 p.u. and the step size is 0.01 p.u.. The range of all nodal voltages is 0.9 ~1.1 p.u.. The voltage regulator tap has a 32-stage adjustment with ± 10% regulation range, the voltage level of load center is 120V, and the bandwidth is 2V.

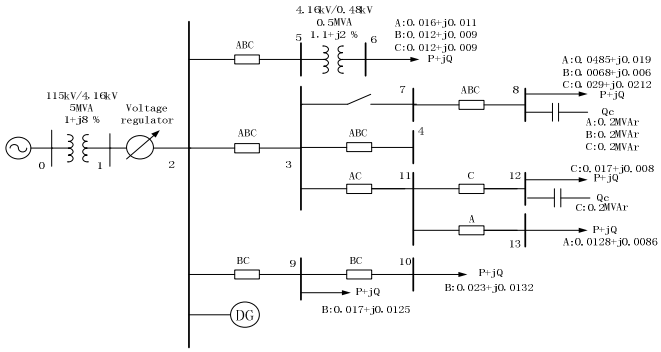

Fig.6. *Modified IEEE13 Test System*

4.1. Analyze the quadratic model of three-phase OLTCs

In order to verify the rationality of the proposed three-phase OLTCs model in the OPF problem for active distribution networks, the OPF calculation based on the predictor-corrector primal-dual interior point method embedding quadratic penalty function (PCPDIPM-QPF) is used to compare the traditional non-quadratic model for three-phase OLTCs [21] and the quadratic model for three-phase OLTCs proposed in this paper. The results are shown in Table 1.

Table 1 The optimization results

	quadratic model of	non-quadratic
Network loss	0.002523	0.002523
Iteration	17	17
Calculating	49.5946	196.8835

Table 1 shows that the results (network loss) of the two methods using different models are the same, but the quadratic model has a faster calculation speed. The reason is that, the Hessian matrix of the non-quadratic model of OLTCs is not constant in the OPF calculation process, and is updated in each iteration, which makes the calculation speed very slow. The quadratic model of OLTCs guarantee a constant Hessian matrix throughout iterations, thus reducing the calculation time greatly.

In addition, the computation time of the two models is relatively long. This is because the Hessian matrix is generated using Matlab's automatic differentiation function, which is convenient but not efficient. This, however, does not affect the conclusion of this paper. The case study involves a total of 17 iterations. The one-time calculation of the Hessian matrix takes 6.67s on the computer with Intel core i3-3240M CPU 3.40GHz, 4GB memory. Therefore, a conservative estimate of the computation time of the non-quadratic model is 17 times of the time for calculating the Hessian matrix, i.e., 113.84s. Therefore, the computation time in Table 1 is justified.

4.2. Analyze the continuous variable discretization process

In order to verify the convergence properties of the quadratic penalty function and the Gaussian penalty function in the OPF calculation, the PCPDIPM-QPF and predictor-corrector primal-dual interior point method embedding Gaussian penalty function (PCPDIPM-GPF) are designed. The OPF for the modified IEEE13 three-phase system is calculated by the two algorithms. This paper proves the advantages and disadvantages of each method by comparing the optimization results (network loss), iteration number and calculating time (the accuracy is e^{-10}).

Table 2 contains the results of the OPF calculation. It shows that, the PCPDIPM-GPF is better than the PCPDIPM-QPF in terms of the optimization results (the network loss is reduced by 2.4%). But the iteration times of the PCPDIPM-GPF is slightly higher than that of the PCPDIPM-QPF, and the PCPDIPM-GPF takes longer time. The reason is that the Gaussian penalty function is a higher order function and the Hessian matrix is a non-constant matrix throughout iterations. So the Hessian matrix is updated as the iterations increasing, which increases the computation time.

Table 2 The optimization results

	PCPDIPM-QPF	PCPDIPM-GPF
Network loss	0.00252	0.00246
Iteration	17	18
Calculating	45.9738	243.2054

Fig.7 shows the comparison of the PCPDIPM-QPF and PCPDIPM-GPF. It can be seen that the dual gap decreases as the iterations increasing, and the time of the PCPDIPM-QPF is about 1/5 of the PCPDIPM-GPF when the convergence effect of the two penalty functions reaches the desired value.

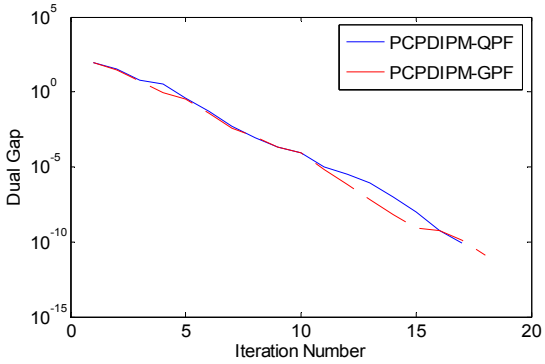

Fig.7. *The optimization results*

4.3. Analyze the integrated regulatory strategy

The integrated regulatory strategy of OPF is implemented by the modified IEEE13 three-phase system with the voltage regulator. It verifies the effect of the voltage regulator on each phase voltages fine-tuning in active distribution networks, and further reduce the network loss in the OPF calculation. The results are shown in Table 3.

Table 3 The optimization results

	Voltage regulator tap			Network loss
	Phase A	Phase B	Phase	
No	—	—	—	0.002523
With	1.006250	1.006250	1	0.002515

As shown in Table III, the network loss of the network with voltage regulator is reduced by 0.32% compared with that without the voltage regulator. The three-phase voltage profile of all nodes, before and after integrated regulatory, is shown in Fig8, Fig9 and Fig10. Thus, the voltage regulator has an effect on fine-tuning the nodal voltages. It can be seen that, the voltage regulator can regulate the nodal voltages at each phase and further reduce the network loss in the OPF calculation.

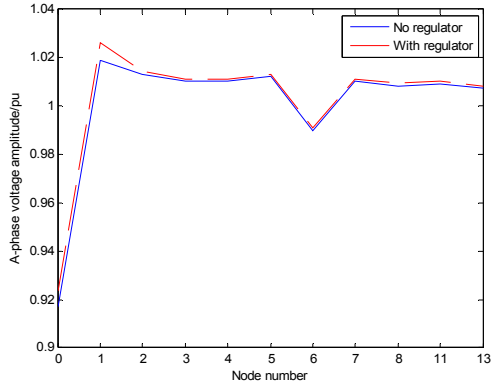

Fig.8. *Voltage profile of phase-A*

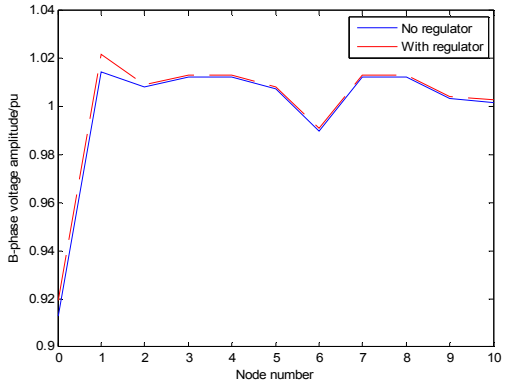

Fig.9. *Voltage profile of phase-B*

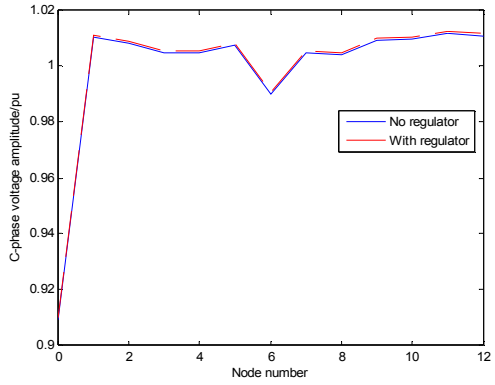

Fig.10. *Voltage profile of phase C*

5. Conclusion

1) This paper proposes a quadratic model for three-phase OLTCs. The model is incorporated into the OPF model, where the Hessian matrix becomes constant throughout iterations. This results in a considerable improvement in computation efficiency.

2) This paper solves the three-phase OPF problem for active distribution networks by using the interior point method. The OPF model incorporates both the quadratic model for the three-phase OLTC (as explained above) and the asymmetric model for the three-phase DG. The methodology is validated by case studies.

3) The case studies demonstrate the advantages and disadvantages of the interior point method incorporating the quadratic penalty function and the Gaussian penalty function.

4) An integrated regulation strategy supported by a voltage regulator is incorporated into the OPF. Case studies demonstrate that the voltage regulator fine-tuned the network voltages, thus further reducing network losses.

6. Acknowledgments

This work was supported by National Key Research and Development Program (2016YFB0900101) and Chinese Universities Scientific Fund (2017QC145).

7. References

[1] E. Sortomme and M. A. El-Sharkawi, ‘Optimal Power Flow for a System of Microgrids with Controllable Loads and Battery Storage,’ in Power Systems Conference and Exposition, 2009. PSCE ’09. IEEE/PES, 2009, pp. 1–5.

[2] Y. Ju, W. Wu, B. Zhang, and H. Sun, ‘Three-phase DFIG steady model and fast three-phase load flow algorithm for distribution power systems,’ in Power System Technology (POWERCON), 2010 International Conference on, 2010, pp. 1–6.

[3] S. Conti, R. Nicolosi, S. A. Rizzo, and H. H. Zeineldin, ‘Optimal Dispatching of Distributed Generators and Storage Systems for MV Islanded Microgrids,’ IEEE Transactions on Power Delivery, vol. 27, no. 3, pp. 1243–1251, Jul. 2012.

[4] Y. Ju, W. Wu, B. Zhang, and H. Sun, ‘An Extension of FBS Three-Phase Power Flow for Handling PV Nodes in Active Distribution Networks,’ IEEE Transactions on Smart Grid, vol. 5, no. 4, pp. 1547–1555, Jul. 2014.

[5] X. Bai, L. Qu, and W. Qiao, ‘Robust AC Optimal Power Flow for Power Networks With Wind Power Generation,’ IEEE Transactions on Power Systems, vol. 31, no. 5, pp. 4163–4164, 2016.

[6] X. Pan, M. Zhou, et al. ‘Impact of Wind Speed Correlation on Optimal Power Flow,’ Automation of Electric Power Systems, vol. 37, no. 6, pp. 37–41, 2013. (in Chinese) .

[7] B. Liu, F. Liu, S. Mei, et al. ‘Optimal Power Flow in Active Distribution Networks with On-load Tap Changer Based on Second-order Cone Programming,’ Automation of Electric Power Systems, vol. 39, no. 19, pp. 40–47, 2015. (in Chinese) .

[8] Y. Liu, W. Wu, B. Zhang. ‘A Mixed Integer Second-order Cone Programming Based Active and Reactive Power Coordinated Multi-period Optimization for

Active Distribution Network,' Proceedings of the CSEE, 2014, 34(16): 2575–2583.

[9] Y. Ju, W. Wu, B. Zhang. 'Three-phase Steady-state Models for Distributed Generators,' Proceedings of the CSEE, 2014, 34(10): 1509–1518.

[10] Y.-C. Wu, A. S. Debs, and R. E. Marsten, 'A direct nonlinear predictor-corrector primal-dual interior point algorithm for optimal power flows,' IEEE Transactions on Power Systems, vol. 9, no. 2, pp. 876–883, May 1994.

[11] A. Sousa, G. L. Torres, and C. A. Canizares, 'Robust Optimal Power Flow Solution Using Trust Region and Interior-Point Methods,' IEEE Transactions on Power Systems, vol. 26, no. 2, pp. 487–499, May 2011.

[12] R. A. Jabr, A. H. Coonick, and B. J. Cory, 'A primal-dual interior point method for optimal power flow dispatching,' IEEE Transactions on Power Systems, vol. 17, no. 3, pp. 654–662, Aug. 2002.

[13] Z. Li, W. Wu, B. Zhang. 'A Large-scale Reactive Power Optimization Method Based on Gaussian Penalty Function With Discrete Control Variables,' Proceedings of the CSEE, vol. 33, no. 4, pp. 68–76, 2013.

[14] J. Yu, W. Yan, G. Xu. 'A New Model of Reactive Optimization Based on Predictor Corrector Primal Dual Interior Point Method,' Proceedings of the CSEE, vol. 25, no. 11, pp. 146–151, 2005.

[15] J. Xu, X. Ding, Z. Qin. 'A Nonlinear Predictor-Corrector Interior Point Method for Reactive Power Optimization in Power System,' Power System Technology, vol. 29, no. 9, pp. 36–40, 2005.

[16] J. Cheng, S. Li, Q. Cheng. 'A Predictor-Corrector Interior Point Method for Optimal Reactive Power,' Transactions of China Electro technical Society, vol. 25, no. 2, pp. 152–157, 2010.

[17] M. Liu, X. Wang. 'An Application of Interior Point Method to Solution of Optimization Problems in Power Systems,' Power System Technology, vol. 23, no. 8, pp. 61–64, 1999.

[18] C. Y. Chung, W. Yan, and F. Liu, 'Decomposed Predictor-Corrector Interior Point Method for Dynamic Optimal Power Flow,' IEEE Transactions on Power Systems, vol. 26, no. 3, pp. 1030–1039, Aug. 2011.

[19] Y. Nie, Z. Du, and J. Li, 'AC-DC optimal reactive power flow model via predictor-corrector primal-dual interior-point method,' IET Generation, Transmission Distribution, vol. 7, no. 4, pp. 382–390, Apr. 2013.

[20] J. Zhao, Z. Hou, S. Ji. 'A Novel Quadratic Penalty Function Based Discretization Algorithm for Newton Optimal Power Flow,' Automation of Electric Power Systems, vol. 23, no. 23, pp. 37–40, 1999. (in Chinese).

[21] W. Wu, B. Zhang. 'Derivation of Detailed Transformer Models and Three-phase Power Flow for Distribution System,' Automation of Electric Power Systems, 2003, 27(4): 53–56.

[22] Y. JU, F. Ge, Y. Lin, J. WANG, 'ADN-Modelica: An Open Source Sequence-Phase Coupled Frame Program for Active Distribution Network Steady State Analysis,' Preprints, 2016.

[23] B. Liang, S. Jin, W. Tang, W. Sheng, K. Liu, 'A Parallel Algorithm of Optimal Power Flow on Hadoop Platform,' in Proc. of IEEE PES Asia-Pacific Power and Energy Conference, pp.1-5, 2016.